Hyperspectral fluorescence lifetime fibre probe spectroscopy for use in the study and diagnosis of osteoarthritis and skin cancer

Alex Thompson*[1], Hugh Manning[1], Mikkel Brydegaard[2], Sergio Coda[1], Gordon Kennedy[1], Rakesh Patalay[1], Ulrika Waitong-Braemming[3], Pieter De Beule[1], Mark Neil[1], Stefan Andersson-Engels[2], Yoshifumi Itoh[4], Niels Bendsøe[5], Chris Dunsby[1], Katarina Svanberg[3], Paul French[1]

[1]*Photonics Group, Dept. of Physics, Imperial College London, London SW7 2AZ, UK*
[2]*Atomic Physics Division, Lund University, SE-22 100 Lund, Sweden*
[3]*Department of Oncology, Lund University Hospital, Lund, Sweden*
[4]*Kennedy Institute of Rheumatology, Imperial College London, London W6 8LH, UK*
[5]*Department of Dermatology, Lund University Hospital, Lund, Sweden*

**Corresponding author: alex.thompson08@imperial.ac.uk*

ABSTRACT

We present the application of two fibre-optic-coupled time-resolved spectrofluorometers and a compact steady-state diffuse reflected light/fluorescence spectrometer to *in vivo* and *ex vivo* studies of skin cancer and osteoarthritis. In a clinical study of skin cancer, 27 lesions on 25 patients were investigated *in vivo* before surgical excision of the region measured. Preliminary analysis reveals a statistically significant decrease in the autofluorescence lifetime of basal cell carcinomas compared to neighbouring healthy tissue. A study of autofluorescence signals associated with the onset of osteoarthritis indicates autofluorescence lifetime changes associated with collagen degradation.

Key words: fluorescence, fluorescence lifetime, diffuse reflectance, osteoarthritis, skin cancer, spectrometer, fibre probe.

1. INTRODUCTION

The intrinsic "autofluorescence" from biological tissue is of interest when studying disease due to the wide range of naturally occurring fluorophores that, through changes in their fluorescence properties, can report on altered metabolism, protein cross links, cell signaling and even disease state [1-7]. In particular the fluorescence lifetime of endogenous fluorophores, which is relatively insensitive to fluorophore concentration and to signal attenuation by the sample, has been shown to effectively differentiate between healthy and diseased tissue, for example in brain tumours, skin cancer and atherosclerotic plaques [7-9]. Accordingly, there is currently much research underway looking into the design and implementation of instruments to measure autofluorescence properties for clinical diagnosis, some examples of which are found in references [10-16]. Besides the potential to provide increased sensitivity and specificity, such instruments could be less invasive and produce faster results than the current gold standard technique of biopsy and histopathology [10].

Here we describe two time-resolved fluorescence spectrofluorometers and a compact steady-state diffuse reflected light/fluorescence spectrometer designed to investigate the clinical diagnostic potential of tissue autofluorescence and present data from an *in vivo* study of skin cancer and an *ex vivo* study of osteoarthritis. The two time-resolved fluorometer systems were developed at Imperial College London and utilise a fibre-optic probe to deliver excitation and collect fluorescence for the parallel measurement of the autofluorescence decay profiles in a number of spectral channels. The compact steady-state diffuse reflected light/fluorescence spectrometer was developed at Lund University and combines measurements of spectrally resolved fluorescence and diffuse reflectance for four excitation wavelengths.

For the *in vivo* study of skin cancer, which was undertaken with 27 lesions on 25 patients at Lund University Hospital, we investigated the diagnostic potential of a dual excitation wavelength hyperspectral fluorescence lifetime

Optical Biopsy IX, edited by Robert R. Alfano, Stavros G. Demos,
Proc. of SPIE Vol. 7895, 78950G · © 2011 SPIE · CCC code: 1605-7422/11/$18 · doi: 10.1117/12.875120

fibre probe [17] and the steady-state diffuse reflected light/fluorescence spectrometer. Such a study is desirable because the methodology used to diagnose skin cancer currently involves a clinical examination by a dermatologist and subsequent histopathology of an excised tissue biopsy. This is both time consuming and invasive and the clinical examination is a subjective procedure that can sometimes lead to the unnecessary removal of benign lesions [10, 18]. Noting that skin cancer is one of the most common forms of malignancy (accounting for nearly half of all cancers in the USA) [19], it seems clear that a non-invasive (optical) method of diagnosis that removed the need for a physical biopsy would be a useful development.

For the study of osteoarthritis undertaken at Imperial College London, the second time-resolved spectrofluorometer was applied to investigate autofluorescence signals from *ex vivo* cartilage tissue. These tissue samples were obtained as porcine trotters or bovine hooves and first processed to extract the cartilage. The purified samples were then treated to simulate the effects of osteoarthritis in terms of collagen degradation. Time-resolved autofluorescence emission spectra were then recorded for each sample in order to investigate whether such autofluorescence signatures of cartilage could be used to detect the onset of disease [20].

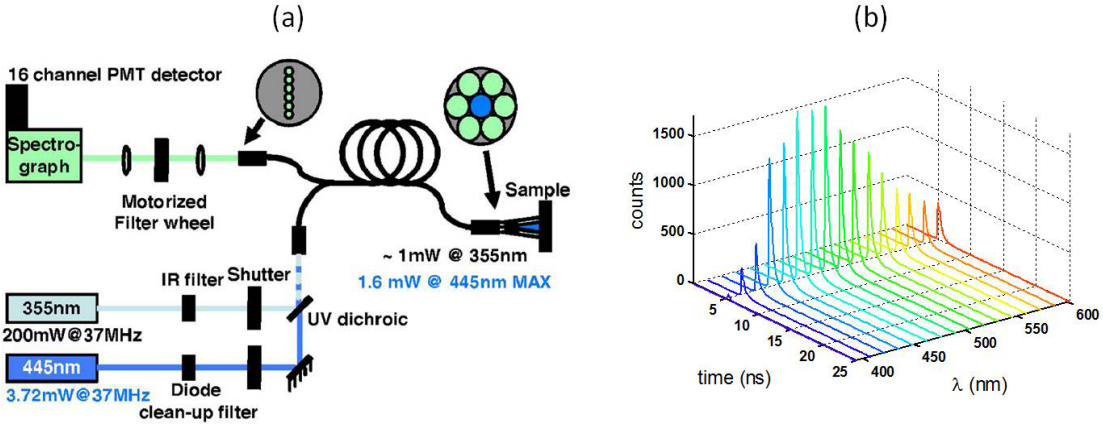

Figure 1. (Colour online) (a) Experimental layout of the fluorescence lifetime fibre probe spectrofluorometer (spectrometer A) and (b) an example of the raw data obtained exciting a solution of NADH with 355 nm radiation. Diagram reproduced, with permission, from (De Beule et al., 2007) [17]. © 2007, American Institute of Physics.

2. INSTRUMENTATION

2.1 Time-resolved fibre-optic probe spectrofluorometer (A)

The first of the two time-resolved spectrometers (A) was developed by De Beule et al. [17]. This system was configured as shown in figure 1(a). Excitation light was provided by two pulsed laser sources – a frequency tripled ultrafast Yb:glass fibre laser (UVPower355, Fianium Ltd., UK), which provided 10 ps pulses at 355 nm with a repetition rate of 37.1 MHz and up to 200 mW of average power, and a diode laser (LDH-P-C-440B, PicoQuant GmbH, Germany), which emitted 50-150 ps pulses at 445 nm with an adjustable repetition rate of up to 40 MHz and up to ~3 mW average power. A maximum power of 10 µW of UV irradiation and 50 µW of blue irradiation was used for the *in vivo* experiments. This radiation was coupled into the excitation channel of a custom built fibre-optic probe (FiberTech Optica, Canada) that comprised seven multimode optical fibres – six for collection of fluorescence and one for delivery of the excitation – each with a core diameter of 200 µm. At the distal end of the probe, the fibres are arranged with the central excitation fibre surrounded by the six collection fibres (inset at top right of figure 1(a)). This arrangement was designed to optimise the illumination and collection efficiency while maintaining a relatively small probe size. At the output to the spectrograph, the six collection fibres are positioned in a line (inset at top centre of figure 1(a)) in order to maximise the coupling into the input slit of the spectrograph. Spectral bandpass filters were employed to clean up the diode emission and to ensure none of the fundamental radiation (at 1.06 µm) from the Yb:glass fibre laser was transmitted to the sample. Computer controlled mechanical shutters in the two beam paths were used to switch between the two excitation sources. The output from the excitation optical fibre was directed onto the sample over an area of ~0.2 mm^2 and the resulting

fluorescence was collected by the six multimode collection fibres which surround the central excitation optical fibre in the FiberTech probe. The output from these collection optical fibres was then imaged onto the input slit of a grating spectrometer (MS125 1/8m, Lot-Oriel, UK) which was attached to a 16 channel multi-anode photomultiplier tube (PMT) detector (PML-16-C, Becker-Hickl GmbH, Germany). The PMT was linked to a computer with a SPC-730 time correlated single photon counting (TCSPC) card running SPCM software (Becker-Hickl GmbH, Germany) so that fluorescence decay profiles could be recorded in 16 spectral channels. Note that a motorised filter wheel was also placed in the beam path between the fibre probe output and the spectrograph to ensure that no stray scattered laser light reached the 16 channel detector. The whole system was mounted on a 60 x 60 cm^2 breadboard to facilitate transportation and fully enclosed for safe use in clinical settings.

A single dataset acquired using this instrument consists of two temporally interleaved sets of 16 spectrally resolved fluorescence decay profiles, one for 355 nm excitation and one for 445 nm excitation. Typically, for each sample we make three identical measurements with each laser with exposure times of around 5 s and so the total acquisition time is on the order of 30 s. An example of the raw data obtained when exciting a solution of NADH with 355 nm excitation is shown in figure 1(b). Before analysis the raw data is corrected to account for the instrument response function of the spectrograph and the non-uniform channel sensitivity of the 16 channel PMT. This was achieved firstly by determining the spectral location of each PMT element using a white light source and a calibrated monochromator and, secondly, by correcting for the intensity in each channel by measuring a known standard [17].

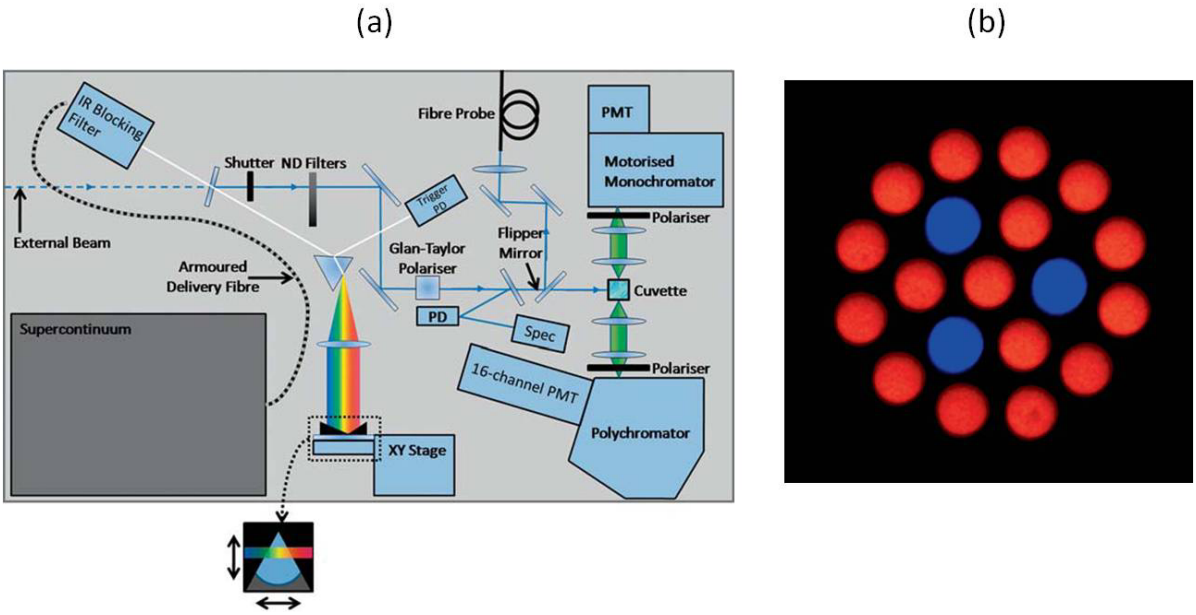

Figure 2. (Colour online) Experimental setup (a) for the multidimensional spectrofluorometer (spectrometer B) and an illustration showing the arrangement of the fibres at the illumination end of the custom fibre probe (b). Blue signifies illumination fibres while red fibres are for collection. Adapted from reference [21]. © Wiley-VCH Verlag GmbH & Co. KGaA. Reproduced with permission.

2.2 Multidimensional fluorometer exploiting supercontinuum generation (B)

The multidimensional fluorometer (B) is also a time-resolved spectrophotometer but incorporates a compact fibre-laser-pumped supercontinuum source (SPC-400, Fianium, UK) to provide picosecond pulses at 20 MHz repetition rate over a wider range (400-800 nm) of excitation wavelengths and can also utilise excitation radiation from an external source if necessary. For the experiments presented here, a diode-pumped frequency-tripled Neodymium Vanadate laser (Vanguard 350-HM355, Spectra-Physics, USA) was used as the external excitation source, which provided 12 ps pulses at 355 nm with 80 MHz repetition rate and up to ~400 mW average power. This fluorometer is able to resolve fluorescence signals using TCSPC with respect to both excitation and emission wavelength and also with respect to polarisation. It can be configured for internal cuvette measurements, as shown in figure 2(a), or for external measurements via a custom-built fibre-optic probe (FiberTech Optica, Canada) that incorporates three excitation fibres and 16 collection fibres, as

depicted in figure 2(b). This external fibre-optic probe, which can be mounted vertically in the same location as the cuvette and uses the same collection optics, was used for the experiments reported here. The fluorometer can switch between two detection arms: one using a spectrograph and a 16 channel TCSPC detector (as described above for spectrometer A) and another with a motorised monochromator (CM110, CVI Inc., USA) and a cooled photomultiplier (PMC-100, Becker-Hickl GmbH, Germany) for single channel TCSPC detection, permitting large spectral regions to be analysed with high resolution [21].

2.3 Wide-field steady-state spectrometer (C)

The third instrument employed for the work described here measures diffuse reflectance spectra and fluorescence spectra with three different excitation wavelengths and was developed at the Atomic Physics Division of Lund University in Sweden. It was specifically designed to be compact and portable and is controlled using software written in Matlab® (MathWorks™) running on a laptop computer. The measurement head, which is represented in figure 3(a), is coupled to a small spectrometer (USB4000, cylindrical lens and second order rejection filter installed, Ocean Optics Inc.) that provides 3 nm resolution and the whole system fits into a small (20x15x15 cm) portable case.

The instrument incorporates seven continuous wave LED sources (Roithner Lasertechnik) comprising a 430 nm LED, a white light LED (Blue+Ce:YAG conversion, 450-700 nm) and two near infrared LEDs (750 nm and 850 nm) for reflectance measurements and LEDs at 355 nm, 375 nm and 395 nm for fluorescence measurements. The emission from the UV LEDs is passed through clean up filters (1mm UG1 or UG11) and each source is directed toward the same central measurement site. The angles of incidence and the use of non-contact optics in the system are designed to minimise specular reflections. For a typical measurement, the sample is illuminated by each source sequentially and the fluorescence or diffuse reflected light passes through a 420 nm long pass emission filter (3 mm GG420) and is collected by a 600 µm diameter optical fibre that delivers the light to the spectrometer. The LEDs and filters are contained within a copper shell, and the thermal dependence of the emissive yield is compensated for by measuring the voltage-current characteristics. Dark spectra are recorded by switching off the sources and these are subtracted from the clinical measurements. The reflectance is calibrated with a 50% grey reference (Oriel) and the fluorescence intensity counts are white calibrated with a filament source (Oriel). In a typical acquisition, the reflectance and fluorescence spectra are recorded at each excitation wavelength in sequence, requiring a total acquisition time of approximately 30 s when averaging over 5 measurements. A graph showing exemplar data of human skin is shown in figure 3(b), which indicates some key features of the spectra. A more complete description of this system can be found in the paper by Brydegaard et al. (2010) [22] where it was used to study fluorescence from bird feathers.

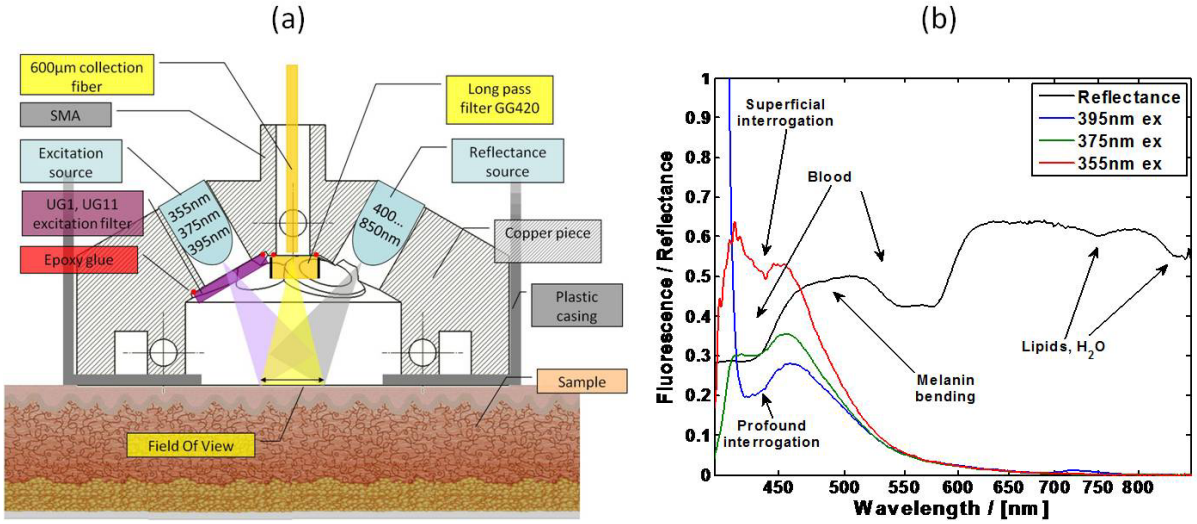

Figure 3. (Colour online) (a) Cross-section through the measurement head of the multi-channel spectrometer (instrument C) and (b) an example dataset from this system – recorded *in vivo* – showing reflectance and fluorescence spectra from human skin.

3. EXPERIMENTAL PROCEDURES

3.1 *In vivo* clinical study of skin cancer

The time-resolved fibre probe (A) and the steady-state wide-field (C) spectrometers were applied together in a clinical *in vivo* study of skin cancer undertaken in the Department of Dermatology at Lund University Hospital. In this investigation, 27 clinically diagnosed skin cancer lesions on 25 patients were examined before excision with the patients being invited to take part in the study after having been clinically assessed by a dermatologist. With the patients' consent, time-resolved measurements of the autofluorescence and steady-state measurements of the autofluorescence and diffuse reflectance were made at the site of each lesion, both in the lesion and in neighbouring "normal" tissue to provide a comparison of their emission and absorption properties. The steady-state spectrometer (C) was applied once to each site while the time-resolved spectrometer (A) was used to make two measurements of normal tissue and one to four measurements within each lesion depending on its size. Afterwards, the entire region irradiated with the fibre probe system was removed and sent to histopathology. Figure 4 illustrates the measurement procedure. Here the filled circles give the positions of the fibre probe measurements on lesion (red), healthy (green) and marginal (orange) tissue. The dotted black circles indicate where the fluorescence and diffuse reflectance spectra were recorded using the steady-state spectrometer. Finally, the dotted red circles indicate the region of tissue that was surgically excised. For each lesion site, the time-resolved fibre probe instrument (A) provided a set of 16 spectrally resolved fluorescence decay profiles for each of the two excitation wavelengths while the steady state spectrometer provided a diffuse reflectance spectrum and an autofluorescence spectrum for each of its three excitation wavelengths.

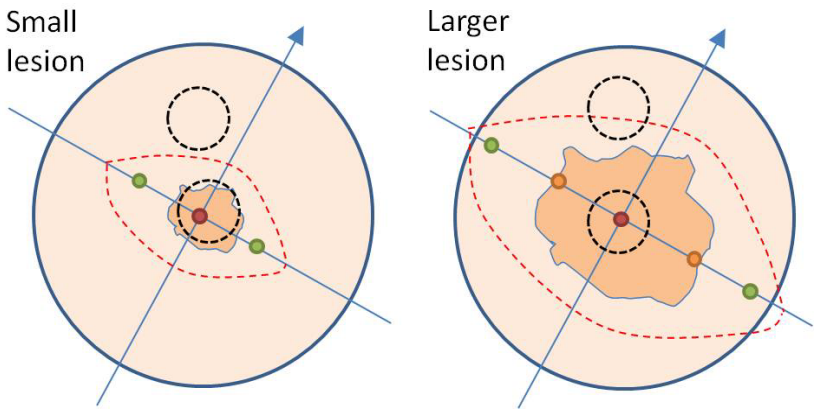

Figure 4. (Colour online) Illustration of the procedure for measuring autofluorescence and reflectance of skin cancer lesions *in vivo*. Both diagrams show a lesion (dark central region) surrounded by healthy tissue (lighter region). The small circles show the location of the fibre probe measurements (red - lesion, green - healthy, orange - marginal), the dotted black circles illustrate where the multi-channel spectrometer was used and the dotted red lines indicate the surgically removed areas.

3.2 Point probe multidimensional fluorescence measurements of cartilage degradation simulating the effects of osteoarthritis

The second study presented here used the multidimensional fluorometer (B) discussed in section 2.2 to study autofluorescence signals from cartilage with a view to investigating their potential for diagnosing tissue degradation due to osteoarthritis. Our methodology was to chemically treat *ex vivo* cartilage samples to simulate the effects of osteoarthritis and to investigate whether the autofluorescence from the tissue could provide information regarding its state of degradation – for which the two main causes are the breakdown of collagen (collagenolysis) and the loss of aggrecan (aggrecanolysis). As collagen is a predominant fluorophore in cartilage, it can be expected that its degradation will affect the autofluorescence signal.

In this study, sections of cartilage excised from porcine trotter joints were excited using 355 nm radiation from a mode-locked frequency-tripled Neodymium Vanadate laser (Vanguard 350-HM355, Spectra-Physics, USA) and time-resolved fluorescence spectra were recorded. Initially normal cartilage was investigated in order to provide a baseline

against which any tissue degradation could be compared. We also compared porcine cartilage to bovine cartilage to assess the differences in autofluorescence from different tissue types. To induce collagenolysis, porcine cartilage was treated with doses of between 0 and 100 µg/ml of bacterial collagenase, thereby simulating one cause of osteoarthritis. Following this treatment, the fluorescence lifetime was measured with an excitation wavelength of 355 nm. Thus, we investigated the effects of the collagenase dose on the autofluorescence signature of the cartilage [20].

4. RESULTS AND DISCUSSION

4.1 *In vivo* clinical study of skin cancer

Steady state spectral measurements

As discussed above, 27 clinically diagnosed cancerous lesions were examined *in vivo* using instruments A and C, (as described in sections 2.1 and 2.3). Figure 5 presents an example of the steady-state spectral data (instrument C) for a specific lesion that was subsequently diagnosed as a basal cell carcinoma (BCC). The graphs show a reflectance spectrum and three fluorescence spectra (one for each excitation wavelength) for the lesion and for adjacent "normal" tissue. The instrument was calibrated as discussed in section 2.3 and so the spectral intensities can be compared across different acquisitions.

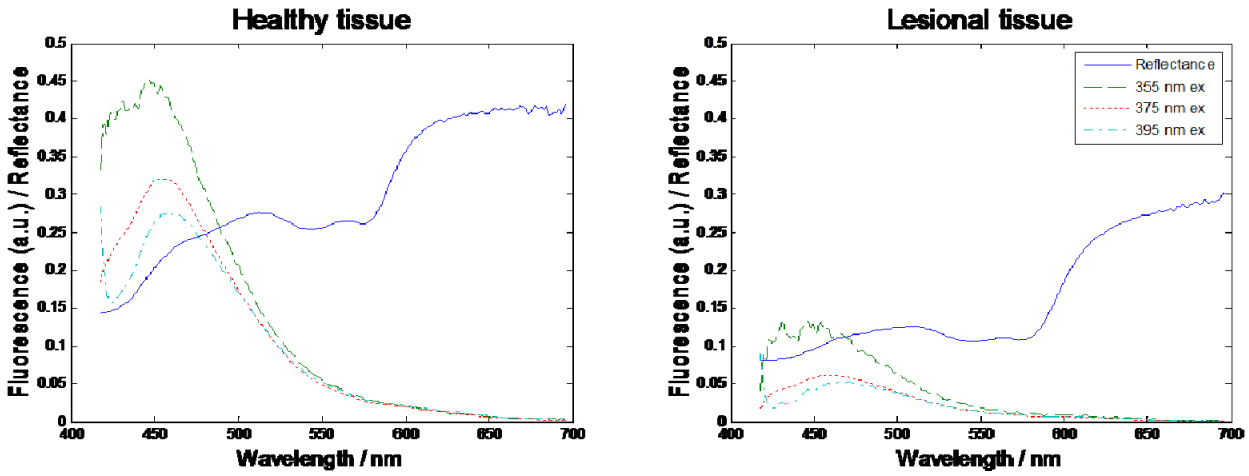

Figure 5. (Colour online) Example spectra from normal (left) and lesional (right) tissue recorded using the steady-state spectrometer (C). Data was taken from a single lesion site where the final diagnosis was BCC. Spectral intensities from different acquisitions can be compared due to the calibration of the instrument discussed in section 2.3.

Figure 5 shows significant differences between the spectra recorded on the lesion and the adjacent normal tissue. We note however, that there was considerable inter-patient variability in the acquired spectra and this is illustrated in figure 6, which shows the mean diffuse reflectance for healthy and diseased tissue for all the measured BCC and actinic keratosis lesions. In these graphs the solid lines show the mean spectra and the dotted lines indicate the standard deviations, with the red (lower) curves corresponding to the lesions and the blue (upper) curves to the normal tissue. For both BCC and actinic keratosis lesions, the mean reflectance is lower than for the surrounding healthy tissue. This trend was observed for all lesion types but we note the significant spread in the data as indicated by the standard deviations. We are currently carrying out a single value decomposition (SVD) analysis of all of the spectra in a method similar to that used by Butte et al. [16] and the results of this analysis will be presented elsewhere. We are also investigating ratiometric analysis in discrete spectral bands and correlating the results with disease type.

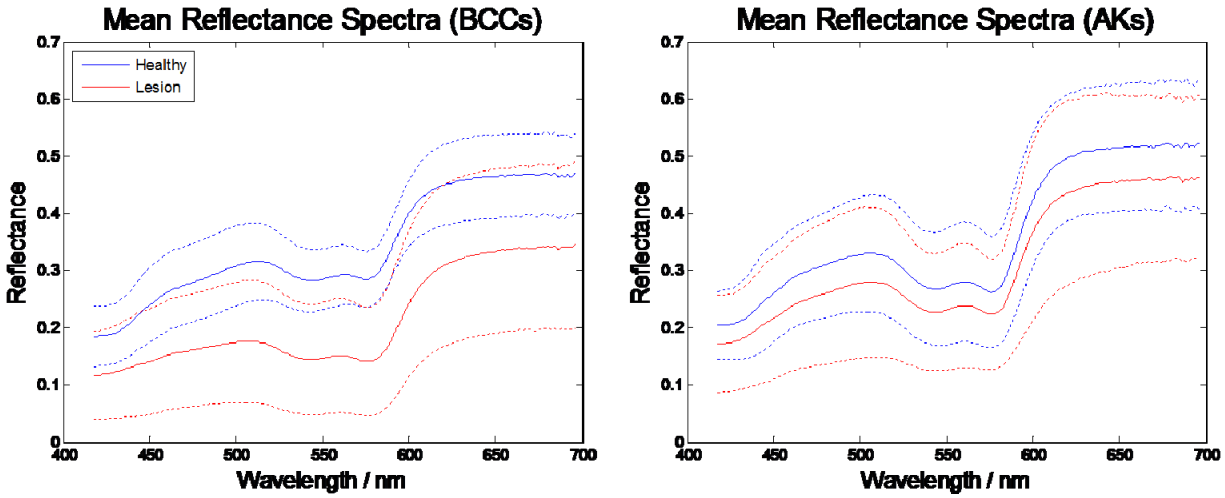

Figure 6. (Colour online) Graphs showing the mean reflectance spectra for all BCC (left) and actinic keratosis (right) lesions. Solid curves show the mean reflectance values and the dotted lines give confidence intervals of ± 1 standard deviation. Blue (upper) lines represent the measurements taken on healthy tissue while the red (lower) curves represent the lesional data.

Time-resolved autofluorescence measurements

Figure 7 shows the data from the time-resolved spectrofluorometer (instrument A). A comparison of the integrated spectra (for 355 nm excitation) was compared to those obtained for the same excitation wavelength using the steady state spectrometer and the two instruments were found to be in good agreement. For the time-resolved data, the fluorescence lifetimes were determined using phasor analysis [23] such that a phase and a modulation lifetime were obtained for each of the 16 spectral channels for each tissue measurement. Figure 7(a) and (b) show the mean emission wavelength for each patient for the normal and lesion measurements. Figure 7(c) and (d) show the mean fluorescence phase lifetime for the same patients. It can be seen that, for 355 nm excitation, there is no clear trend in the mean autofluorescence phase lifetime or mean emission wavelength to distinguish the lesions from normal tissue. For 445 nm excitation, however, there is a clear trend with the lesions exhibiting lower autofluorescence lifetimes than the surrounding healthy tissue in all cases, i.e. $\tau_{lesion} < \tau_{normal}$. A statistical analysis of this data is underway and will be presented elsewhere.

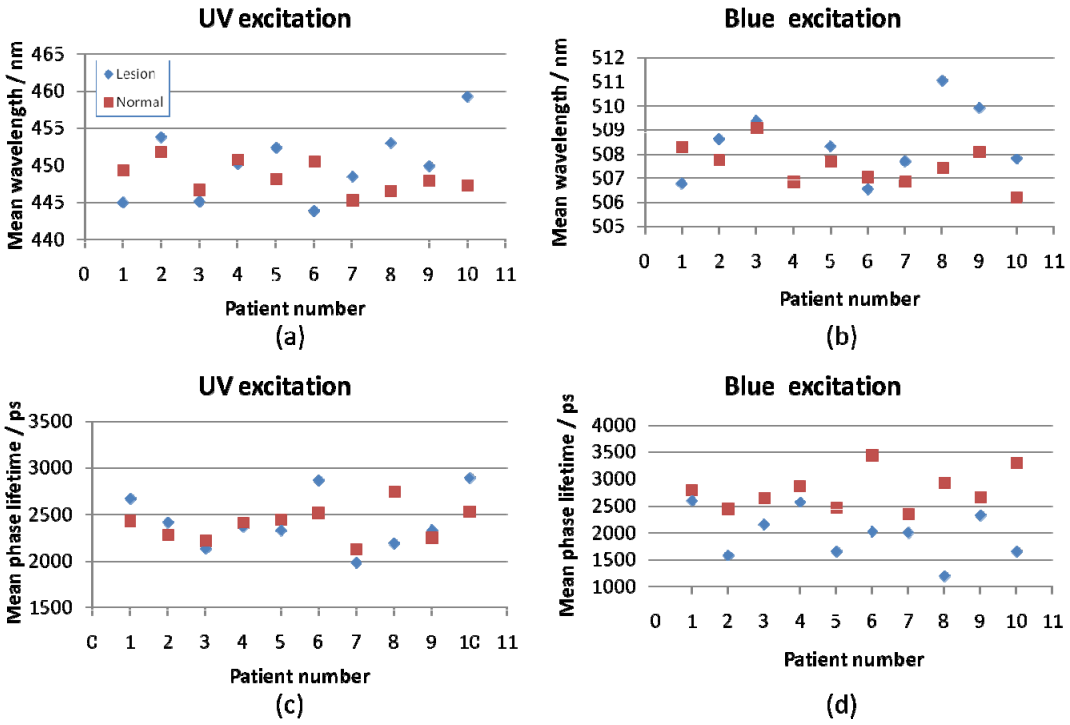

Figure 7. (Colour online) Mean emission wavelength and phase lifetimes for all BCC measurements with UV (left) and blue excitation (right). In (a) and (b), the mean emission wavelength for each patient is given for UV and Blue excitation respectively. In (c) and (d) the mean phase lifetime is given for UV and Blue excitation respectively.

4.2 Multidimensional fluorescence measurements of *ex vivo* cartilage

Fluorescence from normal cartilage

As a first step, an investigation was undertaken to study the emission of normal cartilage. It was observed that cartilage from different sources (i.e. bovine and porcine cartilage) had significantly different autofluorescence lifetimes (data not shown) and that there could be considerable variation from animal to animal. Most of our subsequent studies were undertaken with porcine cartilage with excitation at 355 nm, for which no significant variation of autofluorescence lifetime with emission wavelength was observed and the peak of the emission spectrum occurred at approximately 415 nm. The autofluorescence decay profiles were described well by a double exponential decay model while fitting to a single exponential model produced a much poorer fit to the data [20].

Treatment with bacterial collagenase

A study was undertaken to investigate the effect of degrading cartilage with bacterial collagenase as a convenient model to simulate the cartilage degradation during osteoarthritis. Samples were treated with bacterial collagenase and their autofluorescence was then studied as a function dose. The first studies showed that there was little discernible difference between the emission spectra of a control (untreated) sample and a cartilage sample treated with the collagenase – as shown in figure 7(a). In terms of autofluorescence lifetime, however, a clear trend was apparent. Figure 7(b) shows how the mean autofluorescence lifetime decreased as a function of concentration of bacterial collagenase. For this data, autofluorescence decay profiles at 415 nm were fitted to a double exponential decay model and the mean lifetime was calculated from this fit. This decrease in mean autofluorescence lifetime as a function of increasing dose of collagenase is attributed to a decrease in the lifetime of the long component of the double exponential fit and to an increase in the magnitude of the short component [20].

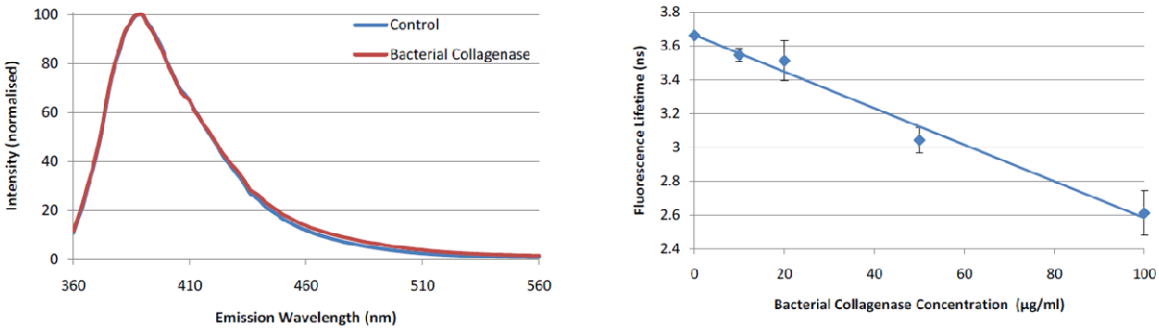

Figure 8. (Colour online) Graphs showing (a) fluorescence spectra from control collagen and collagen treated with 100 µg/ml bacterial collagenase, and (b) the fluorescence lifetime recorded at 415 nm as a function of dose [20].

5. CONCLUSIONS

In this paper we have presented three instruments for the analysis of spectroscopic properties of biological tissue that we have applied to the diagnosis of disease. An ultrafast laser-based time-resolved spectrofluorometer coupled to a fibre optic probe (A) and a compact LED-based steady-state tissue spectrometer (C) have been applied in an *in vivo* clinical investigation of skin cancer at Lund University Hospital. This study, which involved the investigation of 27 lesions, indicated clear differences between healthy and diseased tissue both in terms of spectral properties and autofluorescence lifetime (for excitation at 445 nm), indicating the potential of these instruments for clinical diagnostic purposes. Future work will involve increasing the number of lesions investigated such that it is possible to draw statistically significant conclusions for several individual sub-classes of skin cancer such as squamous cell carcinomas and malignant melanomas.

An investigation was also undertaken of the diagnostic potential of autofluorescence for osteoarthritis. In this preliminary study time-resolved autofluorescence measurements were made of cartilage extracted from porcine trotters using a multidimensional fluorometer (C). When cartilage was treated with bacterial collagenase to simulate the collagen degradation associated with osteoarthritis, a significant decrease in autofluorescence lifetime was observed, while there was no marked change in the emission spectral profile. Further work will be aimed mainly at more accurately simulating the *in vivo* degradation of collagen and also investigating the potential of autofluorescence to read out the loss of aggrecan from cartilage, which is also associated with osteoarthritis.

6. ACKNOWLEDGMENTS

The authors gratefully acknowledge the funding for this work which was provided by the Engineering and Physical Sciences Research Council (EPSRC EP/F040202/1) and the Photonics-4-Life European Network (FP7-ICT-2007-2, 224014). Alex Thompson acknowledges an EPSRC funded PhD studentship and Hugh Manning acknowledges a studentship from the EPSRC-funded Chemical Biology Centre Doctoral Training Centre. Paul French acknowledges a Royal Society Wolfson Research Merit Award.

7. REFERENCES

1. Mycek, M. and Pogue, B. W., [Handbook of Biomedical Fluorescence], Marcel Dekker, (2003)
2. Skala, M. C., Riching, K. M., Bird, D. K., Gendron-Fitzpatrick, A., Eickhoff, J., Eliceiri, K. W., Keely, P. J., and Ramanujam, N., "In vivo multiphoton fluorescence lifetime imaging of protein-bound and free nicotinamide adenine dinucleotide in normal and precancerous epithelia," J Biomed Opt, **12**(2): p. 024014 (2007)

3. Blomfield, J. and Farrar, J. F., "The fluorescent properties of maturing arterial elastin," Cardiovasc Res, **3**(2): p. 161-70 (1969)
4. Fujimoto, D., "Isolation and characterization of a fluorescent material in bovine achilles tendon collagen," Biochem Biophys Res Commun, **76**(4): p. 1124-9 (1977)
5. Thornhill, D. P., "Separation of a series of chromophores and fluorophores present in elastin," Biochem J, **147**(2): p. 215-9 (1975)
6. Eyre, D. R., Paz, M. A., and Gallop, P. M., "Cross-linking in collagen and elastin," Annu Rev Biochem, **53**(717-48 (1984)
7. Marcu, L., Jo, J. A., Butte, P. V., Yong, W. H., Pikul, B. K., Black, K. L., and Thompson, R. C., "Fluorescence lifetime spectroscopy of glioblastoma multiforme," Photochemistry and Photobiology, **80**(1): p. 98-103 (2004)
8. Galletly, N. P., Mcginty, J., Dunsby, C., Teixeira, F., Requejo-Isidro, J., Munro, I., Elson, D. S., Neil, M. A. A., Chu, A. C., French, P. M. W., and Stamp, G. W., "Fluorescence lifetime imaging distinguishes basal cell carcinoma from surrounding uninvolved skin," British Journal of Dermatology, **159**(1): p. 152-161 (2008)
9. Elson, D., Requejo-Isidro, J., Munro, I., Reavell, F., Siegel, J., Suhling, K., Tadrous, P., Benninger, R., Lanigan, P., Mcginty, J., Talbot, C., Treanor, B., Webb, S., Sandison, A., Wallace, A., Davis, D., Lever, J., Neil, M., Phillips, D., Stamp, G., and French, P., "Time-domain fluorescence lifetime imaging applied to biological tissue," Photochem Photobiol Sci, **3**(8): p. 795-801 (2004)
10. Rajaram, N., Aramil, T. J., Lee, K., Reichenberg, J. S., Nguyen, T. H., and Tunnell, J. W., "Design and validation of a clinical instrument for spectral diagnosis of cutaneous malignancy," Appl Opt, **49**(2): p. 142-52 (2010)
11. Kollias, N., Zonios, G., and Stamatas, G. N., "Fluorescence spectroscopy of skin," Vibrational Spectroscopy, **28**(1): p. 17-23 (2002)
12. Lohmann, W., Nilles, M., and Bodeker, R. H., "In situ differentiation between nevi and malignant melanomas by fluorescence measurements," Naturwissenschaften, **78**(10): p. 456-7 (1991)
13. Lohmann, W. and Paul, E., "In situ detection of melanomas by fluorescence measurements," Naturwissenschaften, **75**(4): p. 201-2 (1988)
14. Panjehpour, M., Julius, C. E., Phan, M. N., Vo-Dinh, T., and Overholt, S., "Laser-induced fluorescence spectroscopy for in vivo diagnosis of non-melanoma skin cancers," Lasers Surg Med, **31**(5): p. 367-73 (2002)
15. Sterenborg, H., Motamedi, M., Wagner, R. F., Duvic, M., Thomsen, S., and Jacques, S. L., "In-vivo Fluorescence Spectroscopy and Imaging of Human Skin Tumors," Lasers in Medical Science, **9**(3): p. 191-201 (1994)
16. Butte, P. V., Pikul, B. K., Hever, A., Yong, W. H., Black, K. L., and Marcu, L., "Diagnosis of meningioma by time-resolved fluorescence spectroscopy," J Biomed Opt, **10**(6): p. 064026 (2005)
17. De Beule, P. A. A., Dunsby, C., Galletly, N. P., Stamp, G. W., Chu, A. C., Anand, U., Anand, P., Benham, C. D., Naylor, A., and French, P. M. W., "A hyperspectral fluorescence lifetime probe for skin cancer diagnosis," Rev Sci Instrum, **78**(12): p. 123101 (2007)
18. Mogensen, M. and Jemec, G. B., "Diagnosis of nonmelanoma skin cancer/keratinocyte carcinoma: a review of diagnostic accuracy of nonmelanoma skin cancer diagnostic tests and technologies," Dermatol Surg, **33**(10): p. 1158-74 (2007)
19. American Cancer Society, *www.cancer.org* (2010)
20. Manning, H. B., "Development of multi-dimensional fluorescence metrology and application to cartilage degradation in arthritis," PhD, Imperial College, London, (2010)
21. Manning, H. B., Kennedy, G. T., Owen, D. M., Grant, D. M., Magee, A. I., Neil, M. A., Itoh, Y., Dunsby, C., and French, P. M., "A compact, multidimensional spectrofluorometer exploiting supercontinuum generation," J Biophotonics, **1**(6): p. 494-505 (2008)
22. Brydegaard, M., Lundin, P., Guan, Z., Runemark, A., Akesson, S., and Svanberg, S., "Feasibility study: fluorescence lidar for remote bird classification," Appl Opt, **49**(24): p. 4531-44 (2010)
23. Digman, M. A., Caiolfa, V. R., Zamai, M., and Gratton, E., "The phasor approach to fluorescence lifetime imaging analysis," Biophys J, **94**(2): p. L14-6 (2008)